UDC 620.193.2, 621.793
https://doi.org/10.17073/0021-3438-2024-3-87-96

Research article
Научная статья

High-entropy Fe–Co–Cr–Ni–(Cu) coatings with enhanced corrosion and tribocorrosion resistance obtained by vacuum electrospark deposition

M.N. Fatykhova, K.A. Kuptsov, A.N. Sheveyko, A.R. Gizatullina, P.A. Loginov, D.V. Shtansky

National University of Science and Technology "MISIS"
4 Bld. 1 Leninskiy Prosp., Moscow 119049, Russia

✉ Mariya N. Fatykhova (mariya.antonyuck@ya.ru)

Abstract: High-entropy coatings are highly promising for protecting steel parts in coastal and marine infrastructure from corrosion and tribocorrosion. This study examines the properties of medium- and high-entropy Fe–Co–Cr–Ni–(Cu) coatings produced by vacuum electrospark deposition. The coatings, with thicknesses of up to 30 μm and varying copper content, exhibit a single-phase solid solution structure with an FCC lattice and a dense, homogeneous morphology. The addition of 14 at.% Cu was found to enhance corrosion resistance, shifting the corrosion potential to 100 mV. In friction conditions within artificial seawater, the inclusion of copper also improved tribocorrosion properties, raising the corrosion potential during friction to –165 mV. This improvement is attributed to the galvanic deposition of dissolved copper on the worn areas of the coating, which also reduces the friction coefficient from 0.37 to 0.26. The Fe–Co–Cr–Ni–(Cu) coatings demonstrate high wear resistance, ranging from 5.6 to $9.6 \cdot 10^{-6}$ $mm^3/(N \cdot m)$. The findings confirm the potential of these coatings for applications in environments subject to both friction and corrosion.

Keywords: electrospark deposition, coatings, seawater, electrochemistry, wear resistance, corrosion resistance, tribocorrosion.

Acknowledgments: The research was supported by the Russian Science Foundation, grant No. 20-79-10104-П

For citation: Fatykhova M.N., Kuptsov K.A., Sheveyko A.N., Gizatullina A.R., Loginov P.A., Shtansky D.V. High-entropy Fe–Co–Cr–Ni–(Cu) coatings with enhanced corrosion and tribocorrosion resistance obtained by vacuum electrospark deposition. *Izvestiya. Non-Ferrous Metallurgy.* 2024;30(3):87–96. https://doi.org/10.17073/0021-3438-2024-3-87-96

Высокоэнтропийные покрытия Fe–Co–Cr–Ni–(Cu) с повышенной коррозионной и трибокоррозионной стойкостью, полученные электроискровым легированием в вакууме

М.Н. Фатыхова, К.А. Купцов, А.Н. Шевейко, А.Р. Гизатуллина, П.А. Логинов, Д.В. Штанский

Национальный исследовательский технологический университет «МИСИС»
Россия, 119049, г. Москва, Ленинский пр-т, 4, стр. 1

✉ Мария Николаевна Фатыхова (mariya.antonyuck@ya.ru)

Аннотация: Высокоэнтропийные покрытия представляют большой интерес для защиты стальных изделий, используемых в прибрежной и морской инфраструктуре, от коррозионного и трибокоррозионного воздействия. В данной работе исследованы свойства средне- и высокоэнтропийных покрытий Fe–Co–Cr–Ni–(Cu), полученных методом электроискрового легирования в

© 2024 M.N. Fatykhova, K.A. Kuptsov, A.N. Sheveyko, A.R. Gizatullina, P.A. Loginov, D.V. Shtansky

вакууме. Показано, что покрытия толщиной до 30 мкм с различным содержанием меди характеризуются структурой однофазного твердого раствора с ГЦК-решеткой и плотной, однородной морфологией. Выявлено, что введение 14 ат.% Cu положительно влияет на коррозионную стойкость, смещая потенциал коррозии до 100 мВ. В условиях трения в искусственной морской воде добавление меди также улучшает трибокоррозионные свойства, повышая потенциал коррозии во время трения до –165 мВ. Это обусловлено гальваническим осаждением растворенной меди на изношенные части покрытия, что также положительно сказывается на коэффициенте трения, снижая его с 0,37 до 0,26. Полученные покрытия Fe–Co–Cr–Ni–(Cu) обладают высокой износостойкостью на уровне $(5{,}6\div9{,}6)\cdot10^{-6}$ мм^3/(Н·м). Результаты исследования подтверждают перспективность их использования в условиях трения и коррозии.

Ключевые слова: электроискровое легирование, покрытия, морская вода, электрохимия, износостойкость, коррозионная стойкость, трибокоррозия.

Благодарности: Исследование выполнено за счет гранта Российского научного фонда № 20-79-10104-П.

Для цитирования: Фатыхова М.Н., Купцов К.А., Шевейко А.Н., Гизатуллина А.Р., Логинов П.А., Штанский Д.В. Высокоэнтропийные покрытия Fe–Co–Cr–Ni–(Cu) с повышенной коррозионной и трибокоррозионной стойкостью, полученные электроискровым легированием в вакууме. *Известия вузов. Цветная металлургия*. 2024;30(3):87–96.
https://doi.org/10.17073/0021-3438-2024-3-87-96

Introduction

Due to the active use of marine resources, issues related to the quality and longevity of engineering equipment have become increasingly relevant [1; 2]. Sea water, being an aggressive medium, promotes the development of corrosion in metal parts during their operation [3; 4]. Most moving components of marine and coastal equipment, including pumps, bearings, valves, propellers, gears, etc., are subjected to the synergistic effects of wear and corrosion in sea water — a process known as tribocorrosion. This inevitably accelerates the damage and degradation of mechanical friction units, shortening their service life [5—8]. Additionally, parts that are in a prolonged contact with sea water are prone to biofouling — the growth of microorganisms on the surface, which leads to microbiologically influenced corrosion (MIC) [9]. As a result, the service life is reduced, and energy consumption of engineering equipment increases [10].

Stainless steels with high chromium content (up to 18 %) are widely used for marine equipment components due to the formation of a surface oxide film consisting of Cr_2O_3, which helps reduce corrosion on the surface. Recently, a new type of material, high-entropy alloys (HEAs), has been discovered. These alloys contain passivating elements such as Cr, Ni, Mo, and others, and exhibit superior corrosion and tribocorrosion properties in aggressive environments (sea water, acids) compared to conventional alloys [11; 12]. It is known that copper significantly affects MIC and biofouling by inhibiting the growth and reproduction of microorganisms involved in these processes [13; 14]. However, the introduction of Cu into multi-component Fe—Co—Cr—Ni-based coatings may lead to structural heterogeneity, such as the formation of a two-phase structure (FCC/BCC) or Cu segregation, resulting in the formation of Cu-rich and Cu-deficient zones, and consequently, more intense localized corrosion [15].

A promising application of corrosion-resistant high-entropy alloys is their use as coatings [16]. Economically, the cost of bulk HEAs produced by arc melting or casting is relatively high, considering the addition of expensive alloying elements. However, the deposiiton of coatings helps mitigate this issue. Currently, HEA-based coatings are produced using methods such as laser cladding [17; 18], electrospark deposition [12; 19], magnetron sputtering [20], etc.

Vacuum electrospark deposition (ESD) is a promising method for producing wear- and corrosion-resistant coatings on various steels [21], allowing the formation of “thick” coatings (up to 200 μm) with high adhesion strength due to the micro-welding process between the electrode material and the substrate during deposition. Additional advantages of ESD include its simplicity, the possibility of localized treatment of large parts, and easy automation of the process.

To improve the surface quality and efficiency of electrospark deposition, the process is carried out in a vacuum, which enhances the wettability of the surface by the melt [22]. This effect is associated with the simultaneous occurrence of two parallel processes — pulsed cathodic arc evaporation of the electrode initiated by spark breakdown and classical mass transfer of the electrode material onto the substrate.

The aim of this work is to develop Fe—Co—Cr—Ni—Cu protective coatings with varying copper content using vacuum electrospark deposition to protect steel parts from corrosion and tribocorrosion during operation in sea water.

Materials and methods

Fe—Co—Cr—Ni—Cux coatings with varying copper content were deposited by vacuum electrospark deposition [12]. Discs with a diameter of 30 mm made of 30X13 steel were used as substrates. Electrodes with different compositions (at.%): $Fe_{25}—Co_{25}—Cr_{25}—Ni_{25}$, $Fe_{20}—Co_{20}—Cr_{20}—Ni_{20}—Cu_{20}$ и $Fe_{17.5}—Co_{17.5}—Cr_{17.5}—Ni_{17.5}—Cu_{30}$, were produced by powder metallurgy methods from elemental metal powders using the DSP-515 SA hot-pressing press ("Dr. Fritsch", Germany) at a temperature of 950 °C, a pressure of 35 MPa, and an isobaric hold time of 3 minutes [20].

During the coating deposition process, the pressure in the vacuum chamber was maintained at 20 Pa, the electrode rotation speed was 1000 rpm, and the scanning step and speed were 0.5 mm and 500 mm/min, respectively. To ensure high coating continuity, the scanning direction was changed to perpendicular after each treatment cycle.

The Fe—Co—Cr—Ni—Cux coatings were deposited using the Alier 303 metal electrospark power source (Moldova) with the following technological parameters: pulse current amplitude of 120 (± 20 %) A, pulse frequency of 1600 (± 20 %) Hz, and pulse duration of 40 (± 20 %) μs. The deposition time for each coating was 15 minutes.

The morphology, elemental, and phase composition of the coatings were investigated using scanning electron microscopy (SEM) on an S-3400N microscope ("Hitachi", Japan) equipped with an energy dispersive spectrometer NORAN ("Thermo Scientific", USA), as well as *X*-ray diffraction analysis using a D8 Advance diffractometer ("Bruker", Germany).

The electrochemical properties of the coatings were studied in a three-electrode cell using an IPC Pro MF potentiostat (Russia). A platinum electrode was used as the auxiliary electrode, and an Ag/AgCl electrode, widely used for its simplicity, reliability, and reproducibility of results, was used as the reference electrode. Before the experiments, the coating surfaces were covered with a non-conductive compound to exclude the influence of the substrate material on the electrochemical parameters. The working surface area was 1 cm^2.

The tribocorrosion resistance of the coatings was evaluated using a Tribometer ("CSM Instruments", Switzerland) equipped with a special three-electrode cell that allows the registration of electrochemical corrosion potential during tribological tests in a ball-on-disk configuration. The tests were conducted in artificial seawater at a load of 5 N, a sliding distance of 500 m, and a sliding speed of 10 cm/s. An aluminum oxide (Al_2O_3) ball with a diameter of 6 mm and a roughness of 0.8 μm was used as the counterbody. The wear tracks on the coatings were studied using optical profilometry on a WYKO NT1100 profilometer ("Veeco", USA) [21]. The wear volume of the coatings was calculated according to the method described in [22].

The hardness of the coatings was measured by microindentation on their surface using an automatic microhardness tester DuraScan 70 ("EMCO-TEST Prüfmaschinen GmbH", Austria) by calculating the average value from 10 measurements. The indentation load was 0.01 HV.

Results and discussion

Figure 1 presents SEM images and corresponding element distribution maps of the surface of coatings obtained using Fe—Co—Cr—Ni—Cu_x electrodes (x = 0, 20, 30 at.%) with samples designated as Cu0V, Cu2V, and Cu3V, respectively. All coatings exhibit uniform morphology without visible cracks or chips. According to the element distribution maps, the primary elements (Fe, Cr, and Cu) are evenly distributed (Fig. 1, *b*). The elemental composition of the coatings is provided in Table 1. It can be observed that the iron content is approximately the same, ranging from 39 to 43 at.%. The Cu2V and Cu3V samples contain 14 and 19 at.% copper, respectively, and with increasing copper concentration, the content of Cr, Ni, and Co decreases from 18—21 at.% to 12—16 at.%.

Figure 2 shows SEM images of cross-sections of high-entropy Fe—Co—Cr—Ni—Cu_x coatings. All coatings have dense and a defect-free structure (no cracks or pores). The distribution of Cu across the coating thickness is uniform with a slight decrease from the surface to the substrate (Fig. 2, *b*). As the copper content increases from 0 to 19 at.%, the coating thickness decreases from 30 to 21 μm.

Figure 3 shows the XRD patterns of Fe—Co—Cr—Ni—Cu_x coatings. All samples have a single-phase structure with an FCC lattice based on a solid solution of all metallic elements. Additionally, the structure of the coatings is characterized by a strong texture in the (200) direction, associated with directional crystallization during the solidification of the melt. As the Cu content in the coatings increases, the FCC peaks shift towards lower angles, which is associated with an increase in the lattice parameter from 3.570 to 3.582 Å due to the incorporation of more copper into the cubic phase (see inset in Fig. 3).

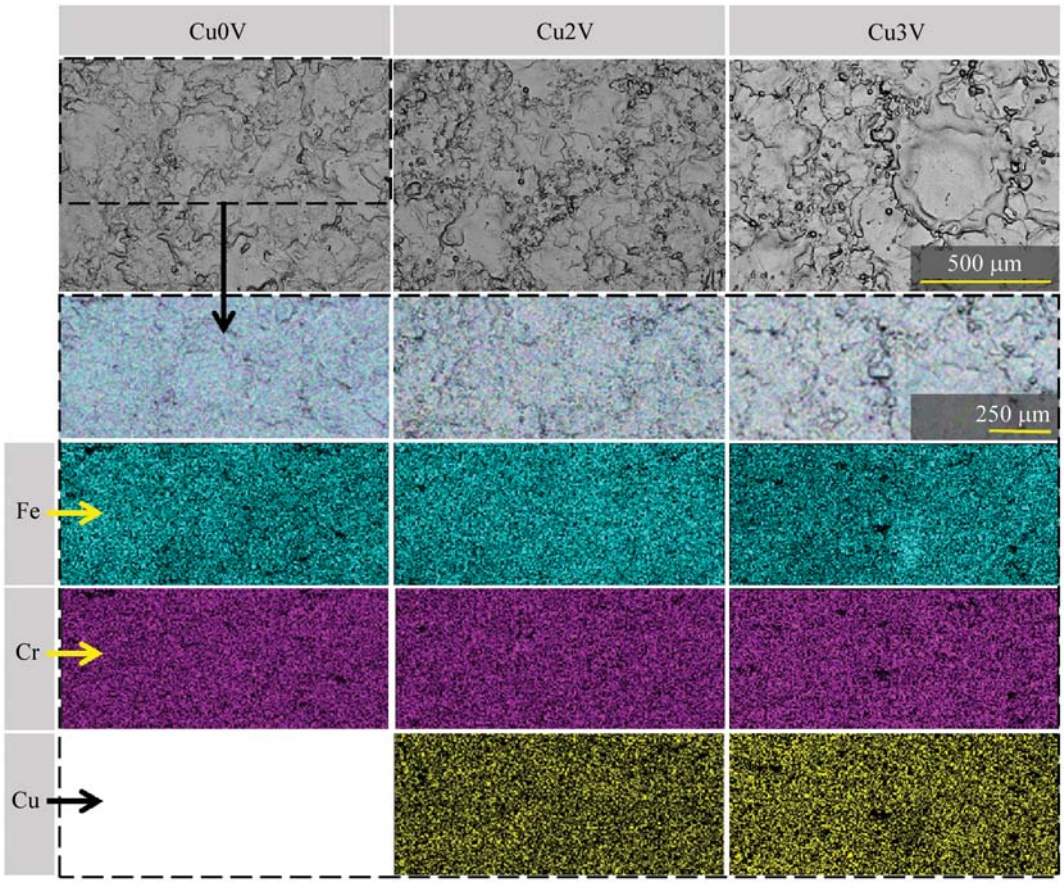

Fig. 1. SEM images of the surface and element distribution maps on the surface of Cu0V, Cu2V, and Cu3V coatings

Рис. 1. СЭМ-изображения поверхности и карты распределения элементов на поверхности образцов покрытий Cu0V, Cu2V и Cu3V

No separate copper-based phases were detected, indicating that all the copper dissolved in the main FCC phase. The crystallite size, estimated using the Debye-Scherrer method, showed minimal influence of copper on this parameter. The introduction of 19 at.% Cu led to a slight decrease in crystallite size from 36 nm (Cu0V) to 34 nm (Cu3V).

To evaluate the corrosion resistance of the coatings, electrochemical tests were conducted in artificial seawater, and the results are shown in Fig. 4. The corrosion potential of the Fe—Co—Cr—Ni coating (sample Cu0V) was +20 mV. The introduction of 14 at.% Cu shifted the corrosion potential in the positive direction to +100 mV, but further increasing the copper concentration to 19 at.% caused a sharp decrease in this value to –150 mV. Interestingly, despite the significant influence of copper on the corrosion potential, the corrosion current density (CCD) of the coatings remained almost unchanged, ranging from 1 to 2 μA/cm^2.

Table 1. **Elemental composition of coatings**

Таблица 1. Элементный состав покрытий

Coating sample	Content, at.%				
	Fe	Co	Cr	Ni	Cu
Cu0V	43	18	21	18	–
Cu2V	43	11	19	13	14
Cu3V	39	12	16	14	19

It is likely that when a certain copper concentration is exceeded, copper accumulates on the surface as iron and other components dissolve. This leads to the formation of individual copper particles, which act as cathodes relative to the surrounding surface. In this case, galvanic pairs form on the surface, leading to partial activation of the metal substrate near the cathodes, which is accompanied by a shift in the zero current potential towards negative values. The influence of these particles on the corrosion current density has two effects. On the one hand, the substrate near the particles dissolves more intensively; on the other hand,

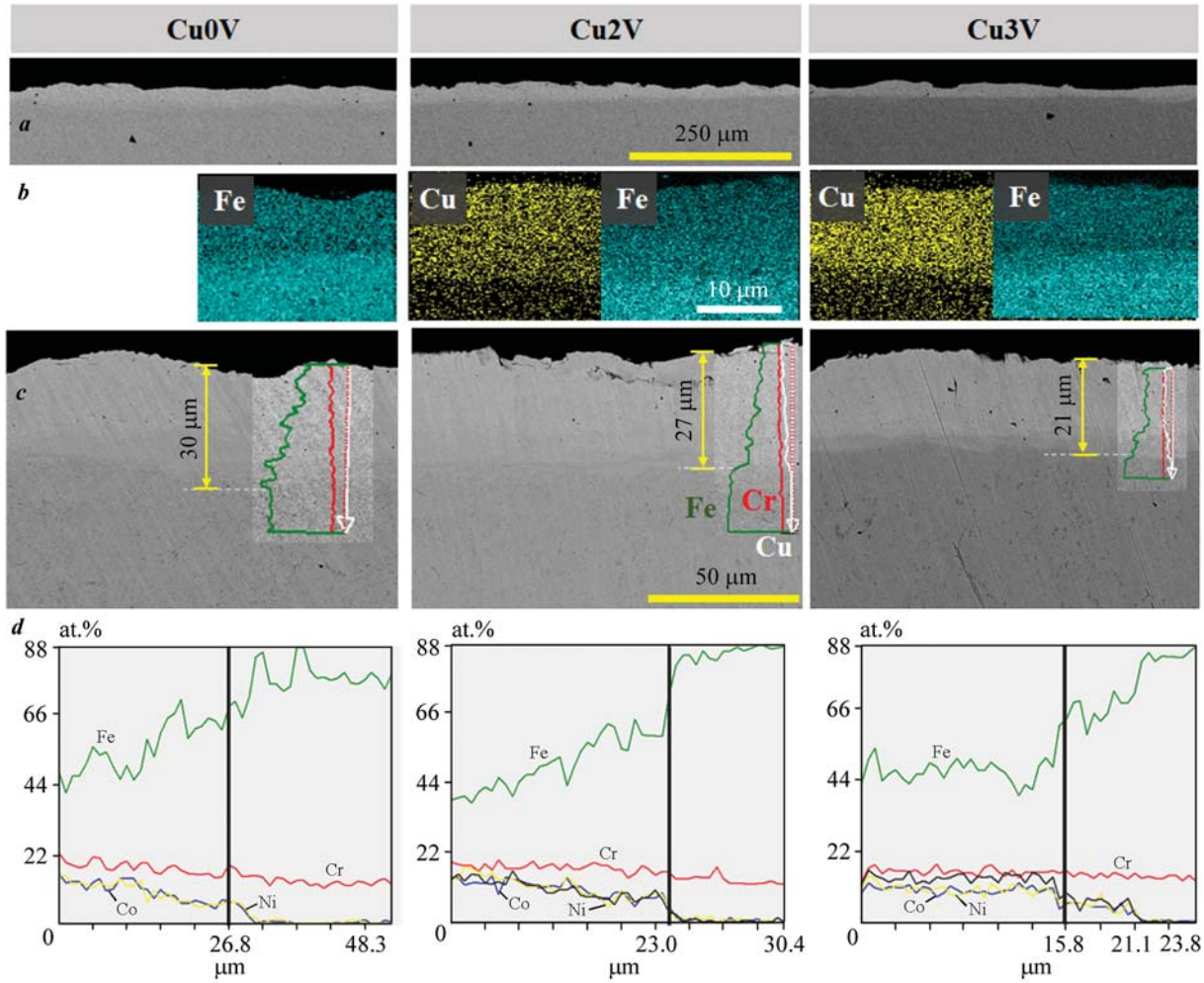

Fig. 2. SEM images of cross-sections of Cu0V, Cu2V, and Cu3V coatings (***a***, ***c***), Cu and Fe distribution maps (***b***), and element distribution profiles (***d***) across the coating thickness

Рис. 2. СЭМ-изображения шлифов покрытий Cu0V, Cu2V и Cu3V (***a***, ***c***), карты распределения Cu и Fe (***b***) и профили распределения элементов (***d***) по толщине покрытия

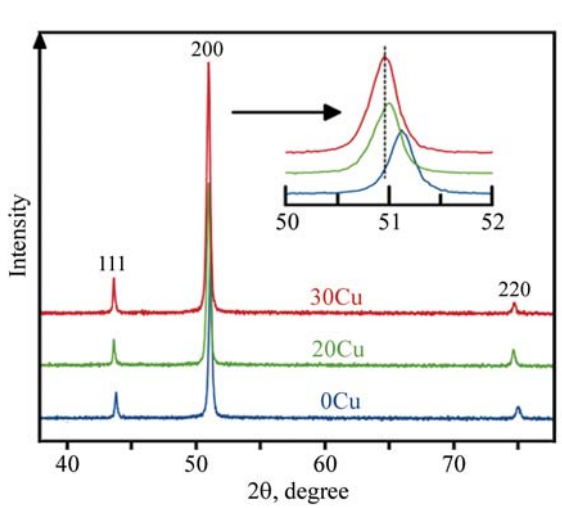

Fig. 3. XRD patterns of Cu0V (***1***), Cu2V (***2***), and Cu3V (***3***) coatings and the (200) peak at higher resolution

Рис. 3. Рентгенограммы покрытий Cu0V (***1***), Cu2V (***2***), Cu3V (***3***) и отдельно пика (200)

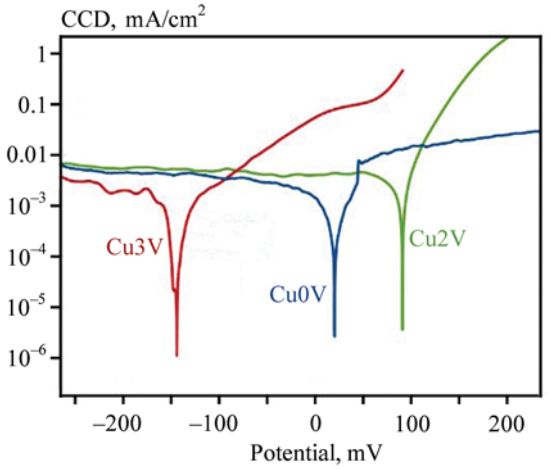

Fig. 4. Corrosion current density versus applied potential for coatings with different copper content

Рис. 4. Кривые зависимости плотности тока коррозии от приложенного потенциала для образцов покрытий с различным содержанием меди

the presence of cathodes promotes better passivation of the matrix in more distant areas. The overlap of these effects leads to the retention of the average CCD at the previous level, although the likelihood of localized corrosion cannot be ruled out.

The synergistic effect caused by the simultaneous impact of wear and corrosion was evaluated through tribocorrosion tests in artificial seawater, during which the electrochemical potential was recorded under both stationary conditions (without friction) and during friction. The experimental results are shown in Fig. 5.

The friction coefficient of the base Cu0V sample monotonically increased from 0.3 to 0.37. The introduction of copper into the coating at 14 at.% (Cu2V) and 19 at.% (Cu3V) led to the stabilization and reduction of the friction coefficient to 0.29 and 0.26, respectively.

When friction started, all coatings experienced a sharp drop in corrosion potential to negative values

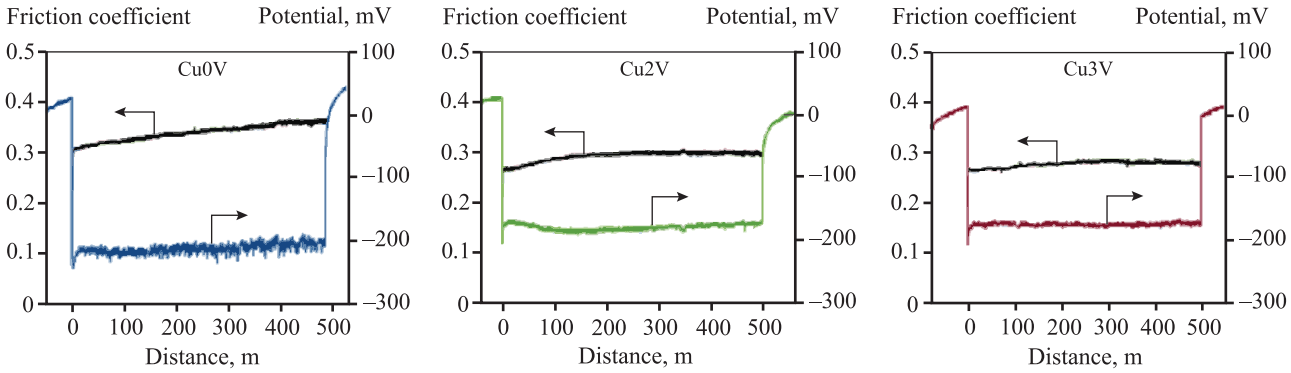

Fig. 5. Tribocorrosion test results of coatings in artificial seawater

Рис. 5. Результаты трибокоррозионных исследований покрытий в искусственной морской воде

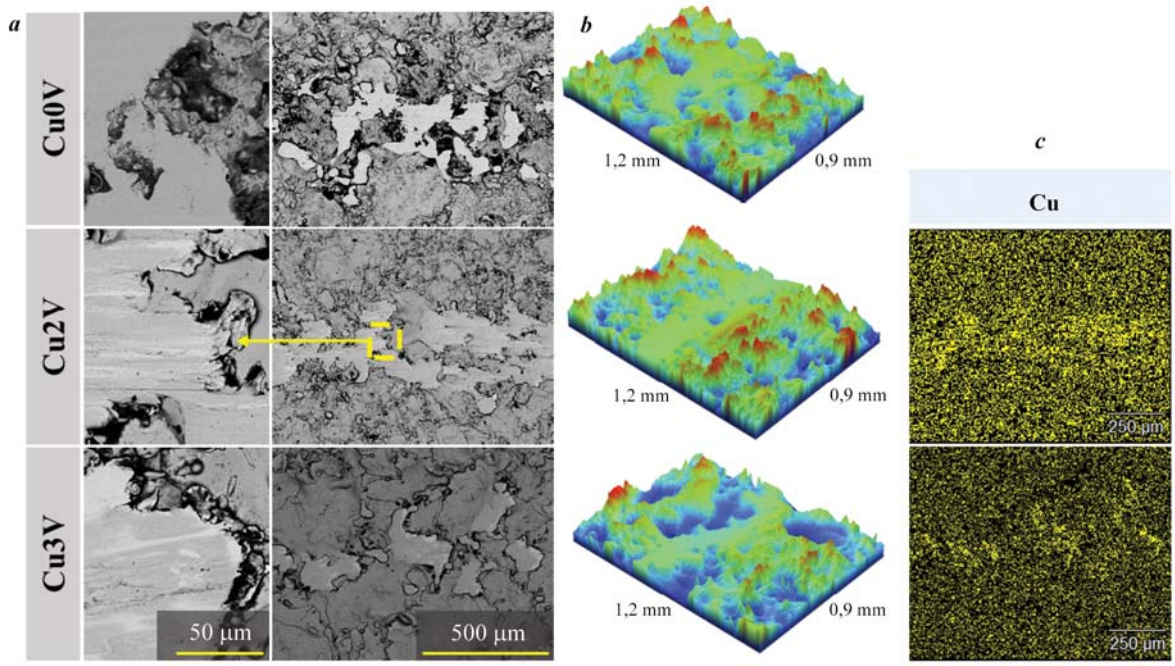

Fig. 6. Wear tracks of Cu0V, Cu2V, and Cu3V coatings

a – SEM images of wear tracks at different magnifications; ***b*** – wear track 3D profiles after tribocorrosion tests; ***c*** – Cu distribution maps in the area of wear tracks

Рис. 6. Дорожки износа образцов покрытий Cu0V, Cu2V и Cu3V

a – СЭМ-изображения дорожек износа при различных увеличениях; ***b*** – 3D-профили дорожек износа после трибокоррозионных исследований; ***c*** – карта распределения меди в области дорожек износа

due to the removal of the protective passive film from their surface. The potential for the Cu0V sample was –200 mV, while for Cu2V and Cu3V coatings, it did not change during friction and remained at –165 mV, indicating more stable tribocorrosion behavior of these samples.

Figure 6 presents SEM images, 3D profiles of wear tracks, and EDS data of Fe—Co—Cr—Ni—Cu_x coatings. The wear tracks of all coatings have similar morphology: partial wear of the surface roughness is observed (Fig. 6, *a*). The areas between the worn regions are filled with wear and corrosion products, mainly consisting of Fe and Cr oxides, as well as residual components of artificial seawater (Table 2).

A unique feature of the tribology of Cu-containing coatings is the accumulation of copper in the wear tracks (Fig. 6, *c* and Table 3). Copper concentrates on the smooth worn areas of the coating due to its galvanic deposition. During corrosion and wear, some copper dissolves into the solution. During friction in the wear track, the surface potential drops significantly below the equilibrium potential for copper dissolution—deposition in this medium. Friction on areas with a worn passive film results in the negative potential, leading to copper deposition in these areas. The accumulation of copper in the wear track results in a reduction of the friction coefficient.

Table 2. **Elemental composition of wear debris in wear tracks**

Таблица 2. Элементный состав продуктов износа в дорожке износа

Coating sample	Content, at.%									
	O	C	Mg	Si	Ca	Cr	Fe	Co	Ni	Cu
Cu0V	45	25	1	1	1	7	15	3	2	–
Cu2V	45	30	1	1	2	3	12	1	2	5
Cu3V	44	27	1	1	1	5	14	3	2	2

Table 3. **Composition of coating and worn surface of the wear track**

Таблица 3. Состав покрытия и изношенной поверхности дорожки

Area	Content, at.%						
	Cr	Fe	Co	Ni	Cu	O	C
Cu0V	17	40	10	11	–	6	16
Wear track	17	41	11	12	–	6	13
Cu2V	14	32	8	9	9	6	22
Wear track	13	28	10	11	18	5	15
Cu3V	14	33	10	12	15	3	13
Wear track	11	26	9	11	24	5	14

Table 4. **Results of tribological tests**

Таблица 4. Результаты трибологических испытаний

Coating sample	Specific wear rate, 10^{-6} mm^3/(N·m)	Hardness, GPa
Cu0V	5.6	2.8
Cu2V	6.3	2.4
Cu3V	9.6	2.3

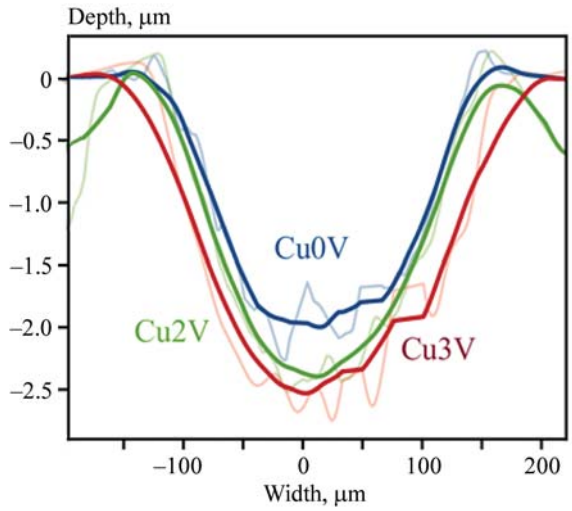

Fig. 7. Profiles of coating wear tracks

Рис. 7. Профили дорожек износа покрытий

To determine the wear rate of the coatings and to exclude the influence of the roughness of the ESD coatings, additional tribological tests were conducted on samples with a polished surface. The results obtained are shown in Fig. 7. It was found that all coatings exhibit high wear resistance; however, with an increase in copper content, the wear resistance slightly decreased from $5.6 \cdot 10^{-6}$ (Cu0V) to $9.6 \cdot 10^{-6}$ (Cu3V) mm^3/(N·m), wich correlates with the hardness that decreased from 2.8 (Cu0V) to 2.3 (Cu3V) GPa (Table 4).

Conclusions

1. Medium- and high-entropy Fe—Co—Cr—Ni—Cu coatings with a thickness of up to 30 μm and varying copper content were obtained by vacuum electrospark deposition. These coatings have a single-phase solid solution structure with an FCC lattice and are characterized by a dense, homogeneous morphology.

2. Under stationary conditions, the introduction of 14 at.% Cu positively affected corrosion resistance, significantly shifting the corrosion potential from +20 to +100 mV. However, further increasing the copper content to 19 at.% negatively affected the corrosion potential, shifting it to —150 mV. The corrosion current density values of all coatings differed slightly, remaining in the range of 1—2 μA/cm^2.

3. During friction in artificial seawater, the addition of copper also positively influenced tribocorrosion properties, allowing the corrosion potential during friction to increase from –200 to –165 mV due to the galvanic deposition of dissolved copper on the worn parts of the coating. The redeposition of copper also positively affected the friction coefficient, reducing it from 0.37 (Cu0V) to 0.26 (Cu3V). Additionally, the Fe—Co—Cr—Ni—(Cu) coatings exhibited high wear resistance in the range of (5.6÷9.6)·10—6 mm^3/(N·m).

References

1. Lu Z., Mao Y., Ren S., Pu J., Fu Z., Fan X., Gao S., Fan J. A novel design of VAlTiCrCu/WC alternate multilayer structure to enhance the mechanical and tribo-corrosion properties of the high-entropy alloy coating. *Materials Characterization*. 2021;176:111115. https://doi.org/10.1016/J.MATCHAR.2021.111115
2. Kuruvila R., Kumaran S.T., Khan M.A., Uthayakumar M. A brief review on the erosion-corrosion behavior of engineering materials. *Corrosion Reviews*. 2018;36:435—447. https://doi.org/10.1515/CORRREV-2018-0022/HTML
3. Feng Z., Huang J., Guo H., Zhang X., Li Y., Fang B., Li Y., Song G.L., Liu J. A magnetic "Band-Aid" incorporated with Fe_3O_4 NPs modified epoxy binder for in-situ repair of organic coating under seawater. *Colloids and Surfaces A: Physicochemical and Engineering Aspects*. 2023;676:132317. https://doi.org/10.1016/J.COLSURFA.2023.132317
4. Liu Z.X., Li Y., Xie X.H., Qin J., Wang Y. The tribo-corrosion behavior of monolayer VN and multilayer VN/C hard coatings under simulated seawater. *Ceramics International*. 2021;47:25655—25663. https://doi.org/10.1016/J.CERAMINT.2021.05.291
5. Usta O., Korkut E. Prediction of cavitation development and cavitation erosion on hydrofoils and propellers by Detached Eddy Simulation. *Ocean Engineering*. 2019;191:106512. https://doi.org/10.1016/J.OCEANENG.2019.106512
6. Shao T., Ge F., Dong Y., Li K., Li P., Sun D., Huang F. Microstructural effect on the tribo-corrosion behaviors of magnetron sputtered CrSiN coatings. *Wear*. 2018; (416-417):44—53. https://doi.org/10.1016/J.WEAR.2018.10.001
7. Niu D., Zhang X., Sui X., Shi Z., Lu X., Wang C., Wang Y., Hao J., Tailoring the tribo-corrosion response of (CrNbTiAlV)C_xN_y coatings by controlling carbon content. *Tribology International*. 2023;179:108179. https://doi.org/10.1016/J.TRIBOINT.2022.108179
8. Ma Y., Li Y., Wang F. The atmospheric corrosion kinetics of low carbon steel in a tropical marine environment. *Corrosion Science*. 2010; 52: 1796—1800. https://doi.org/10.1016/j.corsci.2010.01.022
9. Wang D., Luo H., Zhao S., Tan J., Liang X., Yang J., Zhou S. Seawater-triggered self-renewable amphiphilic coatings with low water swelling and excellent biofilm prevention properties. *Progress in Organic Coatings*. 2013;175:107351. https://doi.org/10.1016/J.PORGCOAT.2022.107351
10. Zhang X., Yu Y., Li T., Wang L., Qiao Z., Liu Z., Liu W. Effect of the distribution of Cu on the tribo-corrosion mechanisms of $CoCrFeNiCu_{0.3}$ high-entropy alloys. *Tribology International*. 2024;193:109401. https://doi.org/10.1016/J.TRIBOINT.2024.109401
11. Wu P., Gan K., Yan D., Fu Z., Li Z. A non-equiatomic FeNiCoCr high-entropy alloy with excellent anti-corrosion performance and strength-ductility synergy. *Corrosion Science*. 2021;183:109341. https://doi.org/10.1016/J.CORSCI.2021.109341
12. Kuptsov K.A., Antonyuk M.N., Sheveyko A.N., Bondarev A. V., Ignatov S.G., Slukin P. V., Dwivedi P., Fraile A., Polcar T., Shtansky D. V. High-entropy Fe—Cr—Ni—Co—(Cu) coatings produced by vacuum electrospark deposition for marine and coastal applications. *Surface and Coatings Technology*. 2023;453:129136. https://doi.org/10.1016/J.SURFCOAT.2022.129136
13. Liu Z., Cui T., Chen Y., Dong Z. Effect of Cu addition to AISI 8630 steel on the resistance to microbial corrosion. *Bioelectrochemistry*. 2023;152:108412. https://doi.org/10.1016/j.bioelechem.2023.108412
14. Zeng Y., Yan W., Shi X., Yan M., Shan Y., Yang K. Enhanced bio-corrosion resistance by Cu alloying in a micro-alloyed pipeline steel. *Acta Metall Sin Engl Lett*. 2022;35(10):1731—1743. https://doi.org/10.1007/s40195-022-01392-9
15. Shi Y., Yang B., Liaw P. Corrosion-resistant high-entropy alloys: A review. *Metals*. 2017;7(2):43. https://doi.org/10.3390/met7020043
16. Zhang C., Lu X., Zhou H., Wang Y., Sui X., Shi Z.Q., Hao J. Construction of a compact nanocrystal structure for (CrNbTiAlV)N_x high-entropy nitride films to improve the tribo-corrosion performance. *Surface and Coatings Technology*. 2022;429:127921. https://doi.org/10.1016/J.SURFCOAT.2021.127921

17. Shon Y., Joshi S.S., Katakam S., Shanker Rajamure R., Dahotre N.B. Laser additive synthesis of high entropy alloy coating on aluminum: Corrosion behavior. *Materials Letters*. 2015;142:122—125. https://doi.org/10.1016/J.MATLET.2014.11.161
18. Jin G., Cai Z., Guan Y., Cui X., Liu Z., Li Y., Dong M., Zhang D. High temperature wear performance of laser-cladded FeNiCoAlCu high-entropy alloy coating. *Applied Surface Science*. 2018;445:113—122. https://doi.org/10.1016/J.APSUSC.2018.03.135
19. Li Q.H., Yue T.M., Guo Z.N., Lin X. Microstructure and corrosion properties of alcocrfeni high entropy alloy coatings deposited on AISI 1045 steel by the electrospark process. *Metallurgical and Materials Transactions A: Physical Metallurgy and Materials Science*. 2013;44:1767—1778. https://doi.org/10.1007/S11661-012-1535-4/FIGURES/15
20. An Z., Jia H., Wu Y., Rack P.D., Patchen A.D., Liu Y., Ren Y., Li N., Liaw P.K. Solid-solution CrCoCuFeNi high-entropy alloy thin films synthesized by sputter deposition. *Materials Research Letters*. 2015;3:203—209. https://doi.org/10.1080/21663831.2015.1048904
21. Sheveyko A.N., Kuptsov K.A., Kiryukhantsev-Korneev P.V., Levashov E.A., Shtansky D.V. Hybrid technology combining electrospark alloying, cathodic arc evaporation and magnetron sputtering for hard wear-resistant coating deposition. *Powder Metallurgy and Functional Coatings*. 2018;4:92—103. (In Russ.). https://doi.org/10.17073/1997-308X-2018-4-92-103
Шевейко А.Н., Купцов К.А., Кирюханцев-Корнеев Ф.В., Левашов А.Е., Штанский Д.В. Гибридная технология осаждения твердых износостойких покрытий, сочетающая процессы электроискрового легирования, катодно-дугового испарения и магнетронного напыления. *Известия вузов. Порошковая металлургия и функциональные покрытия*. 2018;(4):92—103. https://doi.org/10.17073/1997-308X-2018-4-92-103
22. Sheveyko A.N., Kuptsov K.A., Antonyuk M.N., Bazlov A.I., Shtansky D.V. Electro-spark deposition of amorphous Fe-based coatings in vacuum and in argon controlled by surface wettability. *Materials Letters*. 2022;318:132195. https://doi.org/10.1016/J.MATLET.2022.132195

Information about the authors

Mariya N. Fatykhova – Cand. Sci. (Eng.), Junior Researcher of the Scientific-Educational Center of SHS (SHS-Center) of MISIS–ISMAN, National University of Science and Technology "MISIS" (NUST "MISIS").
https://orcid.org/0000-0001-6817-5999
E-mail: mariya.antonyuck@ya.ru

Konstantin A. Kuptsov – Cand. Sci. (Eng.), Senior Researcher of SHS-Center of MISIS–ISMAN.
https://orcid.org/0000-0003-2585-0733
E-mail: kuptsov.k@gmail.com

Aleksanr N. Sheveyko – Researcher of SHS-Center of MISIS–ISMAN.
https://orcid.org/0000-0003-3704-515X
E-mail: sheveyko@mail.ru

Alfina R. Gizatullina – Research Assistant of SHS-Center of MISIS–ISMAN.
E-mail: alfina.gizatullina@yandex.ru

Pavel A. Loginov – Cand. Sci. (Eng.), Senior Lecturer of the Department of Powder Metallurgy and Functional Coatings of NUST MISIS; Senior Research Scientist of the Laboratory "In situ Diagnostics of Structural Transformations" of SHS-Center of MISIS–ISMAN.
https://orcid.org/0000-0003-2505-2918
E-mail: pavel.loginov.misis@list.ru

Dmitriy V. Shtansky – Dr. Sci. (Phys.-Math.), Head of the Research Center "Inorganic Nanomaterials" of NUST MISIS; Chief Researcher of SHS-Center of MISIS–ISMAN.
https://orcid.org/0000-0001-7304-2461
E-mail: shtansky@shs.misis.ru

Информация об авторах

Мария Николаевна Фатыхова – к.т.н., мл. науч. сотрудник Научно-учебного центра (НУЦ) СВС МИСИС–ИСМАН, Национальный исследовательский технологический университет «МИСИС» (НИТУ МИСИС).
https://orcid.org/0000-0001-6817-5999
E-mail: mariya.antonyuck@ya.ru

Константин Александрович Купцов – к.т.н., ст. науч. сотрудник НУЦ СВС МИСИС–ИСМАН.
https://orcid.org/0000-0003-2585-0733
E-mail: kuptsov.k@gmail.com

Александр Николаевич Шевейко – науч. сотрудник НУЦ СВС МИСИС–ИСМАН.
https://orcid.org/0000-0003-3704-515X
E-mail: sheveyko@mail.ru

Альфина Рустемовна Гизатуллина – лаборант-исследователь НУЦ СВС МИСИС–ИСМАН.
E-mail: alfina.gizatullina@yandex.ru

Павел Александрович Логинов – к.т.н, ст. преподаватель кафедры «Порошковая металлургии и функциональные покрытия» НИТУ МИСИС; ст. науч. сотрудник лаборатории «In situ диагностика структурных превращений» НУЦ СВС МИСИС–ИСМАН.
https://orcid.org/0000-0003-2505-2918
E-mail: pavel.loginov.misis@list.ru

Дмитрий Владимирович Штанский – д.ф.-м.н., зав. научно-исследовательским центром «Неорганические наноматериалы» НИТУ МИСИС; гл. науч. сотрудник НУЦ СВС МИСИС–ИСМАН.
https://orcid.org/0000-0001-7304-2461
E-mail: shtansky@shs.misis.ru

Contribution of the authors

M.N. Fatykhova – defined the research purpose and concept, wrote the article, prepared graphic materials, conducted microstructural studies, mechanical and tribocorrosion tests, and discussed and described the results.

K.A. Kuptsov – defined the research purpose and concept, contributed to writing the article, prepared graphic materials, conducted X-ray phase structural analysis, and participated in discussing and describing the results.

A.N. Sheveiko – conducted and described the electrochemical results.

A.R. Gizatullina – contributed to the discussion of research results, prepared graphic materials, and described the results of mechanical tests.

P.A. Loginov – produced the electrodes and contributed to the discussion of research results.

D.V. Shtansky – defined the research purpose and concept.

Вклад авторов

М.Н. Фатыхова – определение цели работы и концепции исследований, написание текста статьи, подготовка графического материала, проведение микроструктурных исследований, механических и трибокоррозионных испытаний, обсуждение и описание результатов.

К.А. Купцов – определение цели работы и концепции исследований, написание текста статьи, подготовка графического материала, проведение рентгенофазового структурного анализа, обсуждение и описание результатов.

А.Н. Шевейко – проведение и описание электрохимических результатов.

А.Р. Гизатуллина – обсуждение результатов исследований, подготовка графического материала, описание результатов механических испытаний.

П.А. Логинов – изготовление электродов, обсуждение результатов исследований.

Д. В. Штанский – определение цели работы и концепции исследований.

The article was submitted 15.04.2024, revised 24.04.2024, accepted for publication 29.04.2024

Статья поступила в редакцию 15.04.2024, доработана 24.04.2024, подписана в печать 29.04.2024